A Scientific Approach to Flame Radiation and Material Flammability

JOHN DE RIS
Factory Mutual Research Corporation
Norwood, Massachusetts 02062, USA

ABSTRACT

The paper briefly reviews our scientific understanding of some of the better understood flammability properties such as ignitability, flame spread, and convective burning to illustrate the utility of practical test method apparatuses for evaluating flammability properties. We then discuss the essential role of flame radiation in controlling hazardous-scale burning rates and why we presently think that a fuel's classical smoke-point may indicate its radiative hazard. We then examine in more detail the soot radiation from small laminar flames to illustrate our emerging scientific understanding of flame radiation. Finally, we suggest a possible smoke-point radiation test apparatus suitable for solid fuels.

INTRODUCTION

The flammability of a material depends on its ease of ignition, ability to propagate a flame, its maximum burning rate per unit surface area and its ease of extinguishment. In general each of these processes depends on different thermo-chemical mechanisms which in turn depend on different combinations of fuel properties as well as the geometric arrangement and scale of the fuel in addition to environmental factors. A central goal of fire research is to develop a series of test methods for evaluating those fuel properties which govern a material's flammability so that one can anticipate and control its fire hazard.

It is now widely recognized that no single material flammability test can completely characterize a fuel's flammability. Instead we need to identify a series of tests which measure the various individual fuel properties controlling flammability. We also need sufficient scientific understanding on how these fuel properties influence fire hazards in different practical situations of interest.

Over the past decade we have made remarkable progress by use of computer models in understanding the progress of fire growth and smoke movement in enclosures and even in complex buildings. However, these models generally presume (rather than predict) the growth rate of the originating fire. We cannot predict fire growth rates, because we lack both a full fundamental understanding of flame radiation and we do not have test methods which measure this essential flammability property.

The present paper briefly reviews our understanding of some of the better understood flammability properties such as ignitability, flame spread, and convective burning to illustrate the utility of practical test methods for evaluating flammability properties. We then discuss the essential role of flame radiation in controlling burning rates and why we presently think that fuel's classical smoke-point may indicate its radiative hazard. We then examine in more detail the soot radiation from small laminar flames to illustrate our emerging scientific understanding of flame radiation. And finally, we suggest a possible smoke-point radiation test apparatus suitable for solid fuels.

SOME ESTABLISHED FLAMMABILITY TEST METHODS

a) Ignitability - Around 1960 basic research on ignition showed that the piloted ignition of a solid could be described by a transient conduction model yielding a time to ignition given by

$$t_{ig} = \begin{cases} \frac{\pi}{4} k_s \rho_s C_s \left(\frac{T_{ig} - T_\infty}{\dot{q}''} \right)^2 & \text{, thermally thick} \\ \rho_s C_s d_s \frac{T_{ig} - T_\infty}{\dot{q}''} & \text{, thermally thin} \end{cases}$$

where $\dot{q}''$ is the net externally imposed heat flux, $T_{ig}-T_\infty$ is the surface temperature rise required for inducing significant fuel vaporization and k_s, ρ_s, C_s and d_s are respectively the solid thermal conductivity, density, specific heat and sample thickness. These simple relationships have readily lead to numerous practical ignition tests for which the time to ignition varies with either the inverse square or inverse first power of applied flux depending on whether the sample is thermally thick or thin. In some cases, such as foamed plastics, thermally thick solids can respond according to the thermally thin formula because of in-depth absorption of the imposed thermal radiation. Because ignition times are sensitive to the wavelength of the imposed radiation it is desirable (but not always practical) to use a long wavelength infrared radiant source characteristic of fires.

b. Flame Spread - Around 1970 basic research on the spread of a creeping flame over a smooth solid surface showed that the spread rate, V, can be described by the simple formulas:

$$V = \begin{cases} \frac{k_g \rho_g C_g V_g}{k_s \rho_s C_s} \left(\frac{T_f - T_\infty}{T_{ig} - T_\infty} \right)^2 & \text{, thermally thick} \\ \frac{\sqrt{2}\, k_g}{\rho_s C_s d_s} \frac{T_f - T_\infty}{T_{ig} - T_\infty} & \text{, thermally thin} \end{cases}$$

where $T_f - T_\infty$ is the flame temperature rise above ambient and V_g is the characteristic buoyancy driven gas-phase velocity near the leading edge of the creeping flame, while k_g, ρ_g and C_g are respectively the thermal conductivity, density and specific heat of the gas phase. More recent research has shown how these spread rates are reduced when local chemical extinction occurs at the leading edge. Also experiments indicate a considerable increase in creeping spread rates with increasing surface roughness.

A comparison of the above flame spread formulas with the previously mentioned ignition relations suggest the interpretation of the flame spread process as a continuous sequence of ignitions for which the creeping flame provides its own local ignition heat flux. This similarity has been exploited by Quintiere and others who correlate ignition times and creeping flame spread rates for a range of external heat fluxes. Such measurements can be made for practical materials on a standard ASTM-E162 apparatus which subjects a material sample to a spatially decreasing heat flux.

c. Convective (Non-Radiative) Burning - During the 1950's and 1960's fundamental theoretical studies on mass transfer and combustion showed that the burning rate per unit surface area of a solid in the absence of flame radiation can be described by

$$\dot{m}'' \cong \frac{h^{(o)}}{C_g} \ln (1 + B)$$

where $\dot{m}''$ is the mass transfer rate per unit area, $h^{(o)}$ is the classical convective heat transfer coefficient associated with the geometry in the absence of mass transfer, C_g is the gas specific heat, and B is the mass transfer driving force which, in the case of convective burning, is given by the ratio

$$B = \frac{\text{Heat release per unit mass of oxidant consumed}}{\text{Heat required to vaporize unit mass of fuel}}$$

The numerator in the above expression is generally quite insensitive to the specific chemistry of typical organic fuels. Thus the mass transfer driving force and consequently the mass transfer rate $\dot{m}''$ depend primarily on the heat of gasification.

Around 1970 this simple result was verified for a variety of small-scale burning situations in which the flames happened to be too small to produce significant flame radiation. Flushed with our apparent sense of success at predicting burning rates several rate-of-heat-release-tests were developed to measure the effective heat of vaporization of practical fuels. Typically such tests impose various levels of external radiative heat flux onto the material sample and measure either: 1) the mass transfer rate by weight loss or 2) the rate-of-heat-release by combustion through the method of oxygen depletion (which exploits the above mentioned proportionality of heat release to oxygen consumed for organic fuels). Typically these tests ignore the heat feedback from the flames to the fuel surface because it is generally considerably smaller than the imposed external radiant heat flux.

Such rate-of-heat-release tests produce valuable fuel property data. For example Pagni[1] and Delichatsios[2] have shown that flame heights correlate very closely with the rate-of-heat-release in both laminar and turbulent situations. Unfortunately, as we discuss below, one cannot infer burning rates of hazardous-scale fires from merely the small-scale rate-of-heat-release tests because they are insensitive (by design) to the flame's own radiation.

RADIATION FROM TURBULENT FLAMES

During the 1970's careful experimental measurements[27] of burning solid fuels revealed that radiative heat transfer from flames generally dominates convective heat transfer for flames larger than - say - 0.20

meters. This important finding has helped explain why the flammability rankings of various fuels are so different at large-scales as compared to small-scales. The burning processes are controlled by fundamentally different heat transfer mechanisms and consequently depend on different fuel properties. Small-scale flames have insufficient heated matter (optical depth) to provide significant radiative heat feedback to the vaporizing fuel surface. On the other hand the enhanced radiation from larger flames causes increased mass transfer rates and a significant decrease in convective heat transfer due to convective blowing away from the surface. This switch-over in burning mechanism was illustrated[3] by comparing the pool fire burning rates of four noncharring plastic fuels: polyoxymethylene (POM), polymethylmethacrylate (PMMA), polypropylene (PP) and polystyrene (PS). These fuels have similar B-numbers (1.23, 1.57, 1.16 and 1.44, respectively) and correspondingly similar small-scale mass transfer rates. However, the sootiness of their flames increases strongly in their listed order so that their theoretical heat release rate increases appreciably at larger-scale, e.g for 30.5 cm square pools, in the sequence 9.34, 24.8, 34.3 and 53.7 kW). The increase in heat release rate is very sensitive to the sootiness of the flames, because the positive radiative heat feedback enhances the burning rate which then increases the flame volume, mean beam length and, in turn, radiative heat feedback.

Typically, about 80% or more of the radiation from luminous flames is emitted by soot while the remaining 20% of the radiation comes from the hot gases such as CO_2, H_2O, CO and unburned hydrocarbons. Modak[4] has developed a convenient and rapid computer program for accurately calculating the radiation along a ray through a homogeneous isothermal gas including soot. Grosshandler[5] and Modak[6] then extended these calculation procedures to nonhomogeneous nonisothermal situations and demonstrated good experimental agreement using time averaged properties for turbulent flames. Modak[7] and others have also shown that the use of Hottel's[8] mean beam length approximations together with zone modeling of major gas volumes generally provide accurate analytical or numerical treatment of geometric effects. We thus have available a solid theoretical framework for predicting flame radiation provided one can estimate the radiation temperatures and soot volume fractions. Such knowledge of flame properties remains as our principal research challenge and is the topic of the rest of this paper.

Numerous measurements of the total radiation from buoyant turbulent fuel jets have shown that the radiant fraction of the heat release, χ_R, is independent of the overall heat release rate and depends only on the thermo-chemical nature of the fuel and surrounding ambient oxidant. It is speculated that this independence of χ_R on Q is due to the fact that the Kolmogorov microscale flow time which is proportional to $Q^{-1/10}/F^{7/5}$ for turbulent fuel jets whose characteristic Froude number F is a constant for purely buoyant jets[9]. Final molecular mixing and combustion takes place at this Kolmogorov microscale.

The radiation from turbulent flames increases strongly with ambient oxygen concentrations because of increasing soot volume fractions. Flames in vitiated atmospheres have reduced radiant fractions[10]. For example, the radiant fraction from a 30 cm diameter PMMA pool fire decreases from 0.36 at an ambient concentration of 20.9% O_2 to 0.25 at 18% ambient O_2. The measured flame radiation temperatures are relatively insensitive to such reductions in ambient oxygen concentrations because of the competing effects of reduced adiabatic stoichiometric flame tem-

peratures and reduced radiant heat loss due to significantly lower soot volume fractions.

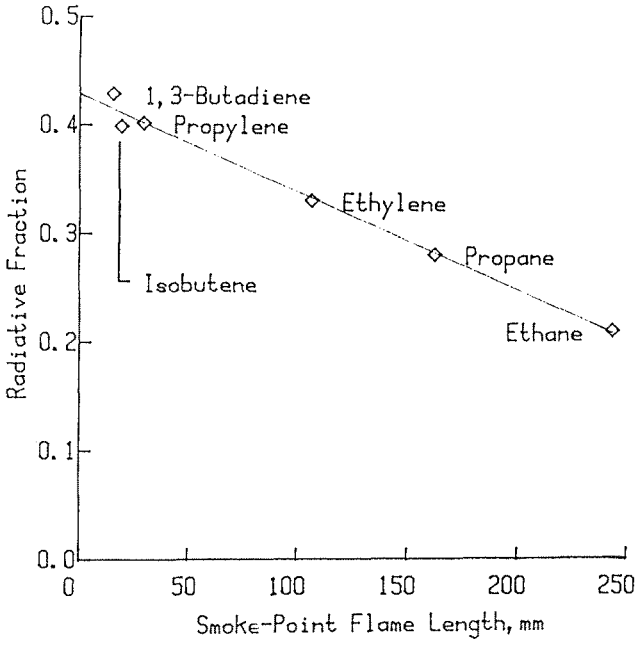

Fig. 1: Radiative fraction χ_{RAD} for turbulent fuel-jet flames of various hydrocarbon fuels vs. smoke-point laminar flame length L_s. Data for L_s taken from Ref. 14.

Figure 1 shows Markstein's[11] recent measurements of radiative fractions from turbulent buoyant fuel jets for various hydrocarbon fuels. Here they are plotted against the classical laminar smoke-point flame heights for the respective fuels. The fuel smoke-point is a measure of its propensity for soot formation. It is defined as the maximum laminar diffusion flame height which just does not release smoke at the flame tip. Sooty fuels have lower smoke-point heights because they lose so much heat by radiation that their flames rapidly cool-off preventing soot oxidation at the flame tip. As can be seen in Figure 1, very sooty fuels have radiant fractions clustering around a maximum of 43%, whereas less sooty fuels such as methane have radiant fractions of less than 20%. Such a twofold change in radiant fraction can have dramatic effects on solid fuel burning rates because of the previously mentioned positive heat feedback role of radiation.

Figure 2 shows Markstein's[12] measurements of the peak soot absorption-emission coefficient (proportional to soot volume fraction) for 0.38 m diameter pool fires having the same 50 kW heat release rate and identical fluid flow fields. Once again we see a correlation with the classical smoke-point values.

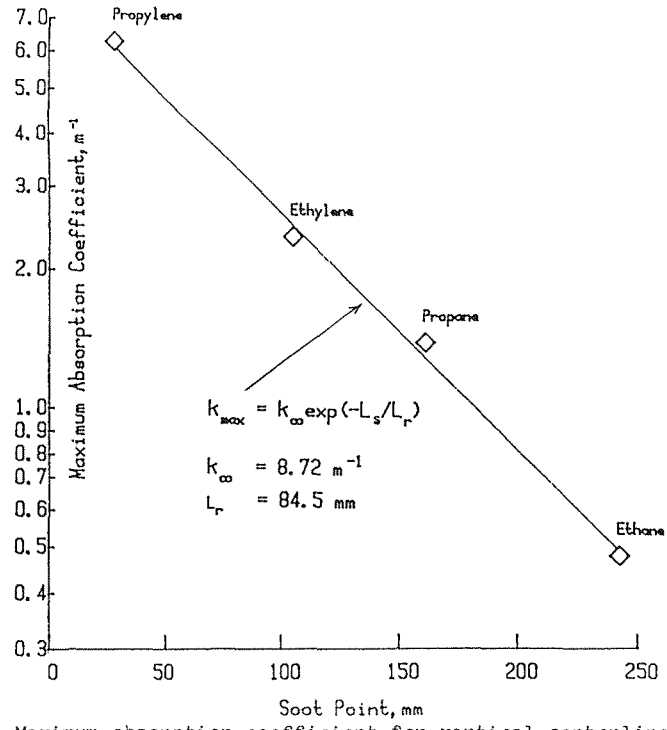

Fig. 2: Maximum absorption coefficient for vertical centerline traverses of 381-mm dia 50 kW fires vs soot-point flame length of laminar diffusion flames (values of L_s taken from Ref. 14).

These two empirical correlations suggest that a fuel's laminar smoke point value apparently has some fundamental relationship to a fuel's large-scale radiation and consequently its large-scale fire hazard. We also have some suspicion that the smoke-point values will correlate the smoke and CO output of a fire; however, this has not yet been experimentally confirmed.

RADIATION FROM BUOYANT LAMINAR FLAMES

To gain deeper fundamental understanding of the relationship of flame radiation and smoke-point, we shall now review some recent results for laminar buoyant flames.

a) Laminar Flame Heights - We first shall derive a general formula for the height of a small buoyant laminar flame issuing from a circular orifice. Experiments show that the flame height is proportional to the fuel supply rate and independent of the orifice diameter. In general for buoyant laminar boundary layer flows the characteristic upward velocity u_f, and characteristic flame radius r_f, adjust themselves to satisfy the momentum and continuity equations resulting in approximately equal buoyancy, inertia and viscous forces per unit height. Define the force ratios

$$F^2 = \frac{[\rho_f u_f^2 \pi r_f^2/\ell_f]}{[(\rho_\infty - \rho_f) g \pi r_f^2]} = \frac{\rho_f u_f^2}{(\rho_\infty - \rho_f) g \ell_f}$$

$$R = \frac{[\rho_f u_f^2 \pi r_f^2/\ell_f]}{[\rho_f \nu_f (u_f/r_f) 2\pi r_f]} = \frac{u_f r_f^2}{2 \nu_f \ell_f}$$

where ℓ_f, ν_f and ρ_f are respectively the overall flame length, flame kinematic viscosity and flame density. We anticipate that both F^2 and R are of order of unity for our buoyancy controlled flames. Solving for u_f and r_f, one has

$$u_f = [F(\rho_\infty - \rho_f) g \ell_f/\rho_f]^{1/2} \quad , \quad r_f = [4R^2 \nu_f^2 \ell_f \rho_f / F(\rho_\infty - \rho_f) g]^{1/4} \qquad (1a),(1b)$$

showing that u_f and r_f scale respectively with the second and fourth roots of height as is characteristic of upward laminar buoyant flows.

Approximating the diffusion flame shape by a right circular cylinder, one obtains the overall (undiluted) fuel mass consumption rate, $\dot{M}_F$, as

$$\dot{M}_F = \dot{m}''_F \, 2\pi r_f \ell_f \qquad (2)$$

Here $\dot{m}''_F$ is the mean fuel mass consumption rate per unit flame area, which can be estimated from the variable property solution[9] for a planar diffusion flame in a flow field undergoing a uniform straining deformation, u_f/ℓ_f, given by

$$\dot{m}''_F = \rho_f D_f \frac{\partial Y_F}{\partial r_f}\bigg|_{r_f} = \frac{Y_{FT}}{s} \rho_f (u_f D_f/8\ell_f)^{1/2} G(s) \qquad (3)$$

where Y_{FT} is the mass concentration of fuel issuing from the burner port, $s = Y_{FT}\nu'_O M_O / Y_{O\infty}\nu'_F M_F$ is the stoichiometric mass of oxidant required by unit mass of burner gas, D_f is the species diffusivity, while G(s) is a weak function of s equal to $5 \pm .5$ for $6 \leqq s \leqq 15$.

Solving for ℓ_f between Eqs. (2) and (3), and then substituting from Eqs. (1a) and (1b) for u_f and r_f, one obtains the general equation for flame height,

$$\ell_f = \frac{\dot{M}_F s}{\pi Y_{FT} G(s) \rho_f (D_f \nu_f R)^{1/2}} = \frac{\dot{M}_F s}{\pi Y_{FT} G(s) \rho_\infty (D_\infty \nu_\infty R)^{1/2}} \left(\frac{T_\infty}{T_f}\right)^{3/4} , \qquad (4)$$

after considering the well-known temperature dependence, $\frac{D_f}{D_\infty} = \frac{\nu_f}{\nu_\infty} = \left(\frac{T_f}{T_\infty}\right)^{7/4}$.

Roper[13] obtained a similar formula with G(s) replaced by $4s\ell n(1+1/s)$ for the flame height above a circular port. Note that $\dot{M}_F$ is the supply rate of actual fuel and that s/Y_{FT} is independent of Y_{FT} so that ℓ_f is independent of Y_{FT} except very weakly through G(s). This formula with R=1 agrees within 5 percent with the available experimental data[14-17] involving a wide range of fuel and oxidant compositions, thus justifying the assumptions underlying Eqs. (1a, 1b). Although neither g nor F appear in the flame height formula, its assumptions presuppose a buoyancy driven boundary layer flow. Thus it is not valid at zero g.

b) Soot Scaling Relationships - Recently Markstein and de Ris[18] measured the flame absorption and soot absorption cross-sections per uni height for buoyant laminar flames from ethylene and propylene which hav significantly different smoke-point values as seen in Figure 1. Thes data are correlated in Figure 3 for soot plus gas radiation, and in Fig ure 4 for soot alone. For all flames, soot cross-sections correlate i the lower soot- formation regions. For flame heights less than th smoke-point values, the soot cross-sections also correlate in the uppe soot-oxidation region. For flame heights above the smoke-point value the correlations break down because the radiant heat loss from the flame cause a reduction in soot oxidation rates and a release of unburned soo from the flame tip.

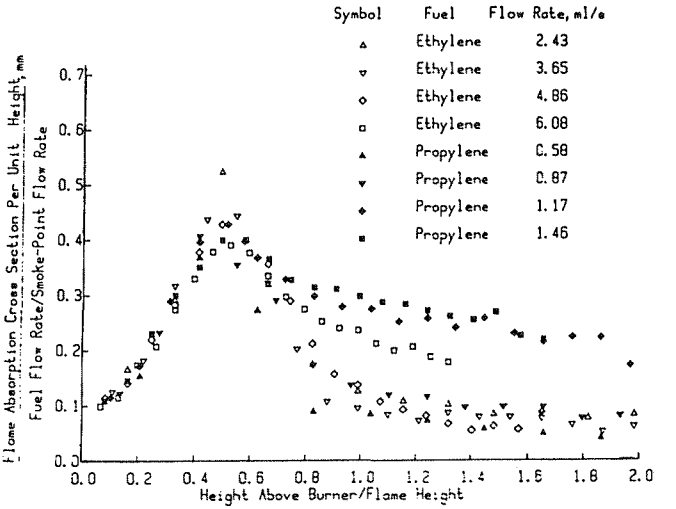

Fig. 3: Normalized plot of spectrally flat absorption cross sections fo laminar diffusion flames

This study also reveals that at a height equal to the smoke-poin flame length, the flame temperature is 1600K for both fuels. Apparently soot oxidation rates are significantly reduced at this temperature Olson[19] also found that the characteristic flame temperatures of hydro carbon fuels are nearly identical for flames at their smoke-point condi tion.

Figures 3 and 4 show that the peak values of soot absorption per uni height, $a_s = \pi k_s r_f^2$ increase linearly with fuel flow rate and have th same peak value ($\sim$ 1 mm) for both ethylene and propylene at their respec tive smoke-points, that is

$$(\pi k_s r_f^2)_{peak} \sim \ell_f/\ell_{fs}$$

Since both r_f^2 and the characteristic flow time, $\tau_f = \ell_f/u_f$ are propor tional to $\ell_f^{1/2}$, the data suggest the following scaling of the soot for mation rate

$$\frac{Dk_s}{Dt} = \frac{(k_s)_{peak}}{\tau_f} = \frac{(k_s r_f^2)_{peak}}{\tau_f r_f^2} \sim \frac{(\ell_f/\ell_{fs})}{\ell_f} \sim 1/\ell_{fs} \qquad (5$$

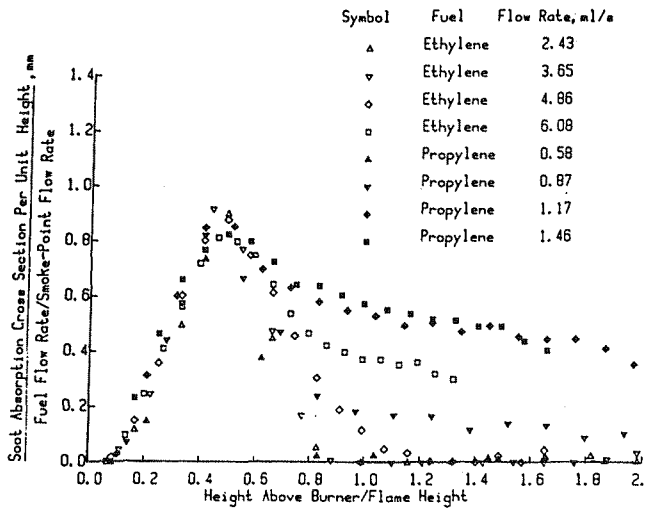

Fig. 4: Normalized plot of monochromatic absorption cross sections for laminar diffusion flames

which is independent of the flame height, ℓ_f, for a given fuel. Thus the overall soot formation rate scales in a simple manner despite the considerable complexities of the detailed processes. Furthermore, for flames at their smoke points $\tau_f = \tau_{fs} \sim \ell_{fs}^{1/2}$ provides

$$(k_s)_{soot\text{-}point} = \tau_{fs} \frac{Dk_s}{Dt} \sim 1/\ell_{fs}^{1/2} \tag{6}$$

which is consistent with $(k_s r_f^2)_{peak}$ being equal at the respective smoke points.

This result allows one to estimate the overall radiative fraction, χ_R, from these flames at their respective smoke points.

$$\chi_{Rs} = \dot{Q}_R/\dot{Q}_{TOT} = 4\pi k_s \sigma (T_{fs}^4 - T_\infty^4)(\pi r_f^2 \ell_f)/\dot{M}_F \Delta H_c \tag{7}$$

where $4\pi k_s \sigma(T_{fs}^4 - T_\infty^4)$ is the effective radiation per unit flame volume and $(\pi r_f^2 \ell_f)$ is the flame volume. Since: 1) the flame temperatures T_f are the same at the respective smoke points; 2) $\ell_f \sim \dot{M}_F$ for similar flame temperatures and stoichiometries; and 3) $(k_s r_f^2)_{peak}$ is the same for fuels at their respective smoke points, we anticipate that the two fuels, ethylene and propylene, should have identical overall radiative fractions at their smoke points. This result was predicted prior to measurement of the overall radiative fractions from laminar diffusion flames. Its confirmation, as described below, adds considerable reinforcement to the concept of fundamental role of the smoke- point for characterizing both soot-formation rates and flame radiation.

c) Radiative Fraction from Laminar Flames - Figure 5 shows Markstein's[11] correlation of the overall radiative fraction for four olefin fuels versus their heat release rate, $\dot{Q}_T$, normalized by its smoke-point value $\dot{Q}_{TS}$. [Here $\dot{Q}_L$ is a small empirical correction for: 1) heat loss

to the fuel holder, and 2) blue zone quenching taking place at the flam base. Theoretical arguments, data and visual observations suggest tha this small correction is independent of the fuel supply rate.] This re markable correlation spans a wide range of heat release rates. We not that the four fuels have similar adiabatic stoichiometric flame tempera tures (~ 2300 K).

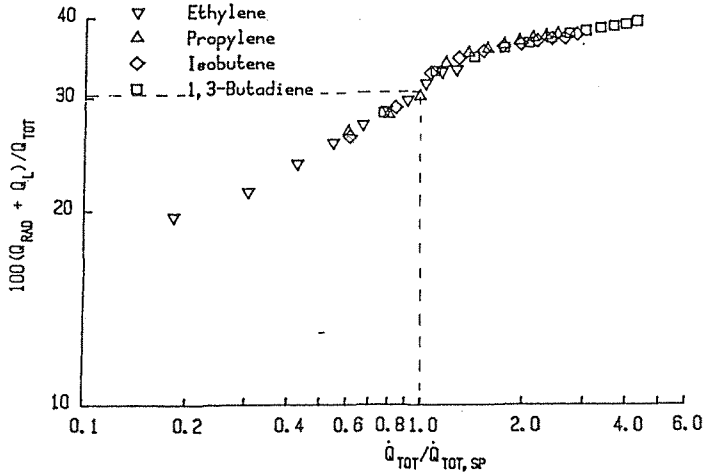

Fig. 5: Total loss fraction vs. total heat release rate normalized b the smoke-point value, for laminar diffusion flames ($\dot{Q}_L$ 2.91W). For greater clarity only every third data point ha been plotted. Dashed lines indicate smoke point.

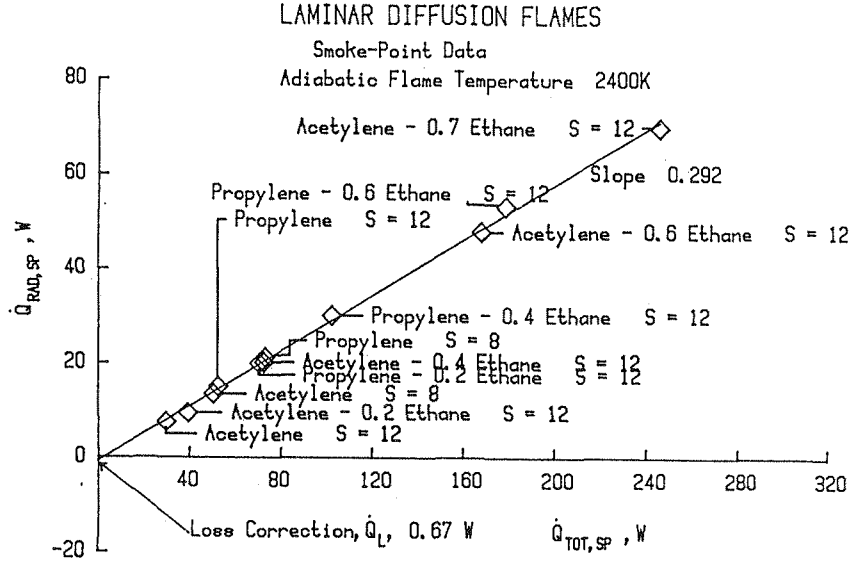

Fig. 6: Smoke-point radiant output for a variety of fuel/oxidant combi nations having an adiabatic stoichiometric flame temperatur equal to 2400K. Here S is the stoichiometric oxidant/fuel mas ratio.

Figure 6 shows the smoke-point radiant output for a variety of fuel/oxidant combinations whose compositions are adjusted to produce identical adiabatic stoichiometric temperatures equal to 2400 K, but with a variety of compositions and stoichiometric oxidant/fuel mass ratios, s. It is apparent from this figure that the smoke-point radiant fraction is independent of the stoichiometric mass ratio and fuel/oxidant chemistry at a fixed theoretical flame temperature. Similar results were obtained for theoretical flame temperatures of 2200 K and 2600 K. These results are summarized in Figure 7. We thus conclude that the smoke-point radiant fraction from buoyant laminar diffusion flames depends only on their adiabatic stoichiometric flame temperature.

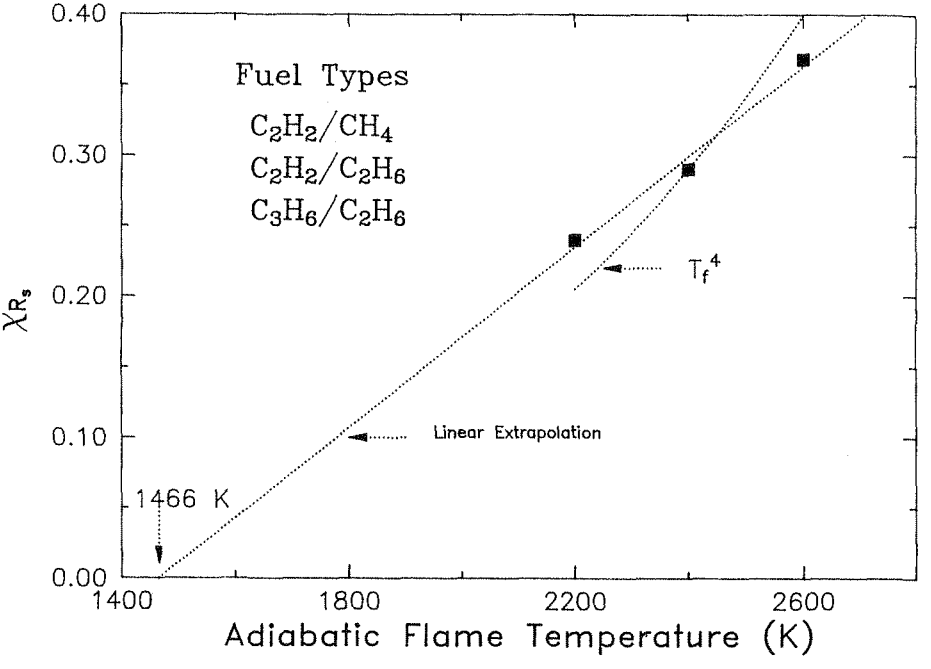

Fig. 7: Summary of smoke-point radiant fraction data for adiabatic flame temperature equal to 2200, 2400 and 2600 K. Note deviation from T^4 curve.

d) Soot Absorption for Smoke-Point Flames - Figure 8 shows Olson's[19] measurements of the mid-height soot volume fractions for a wide variety of hydrocarbon fuels burning in air at their respective smoke points. The abscissa is his so-called threshold sooting index (TSI) which is essentially inversely proportional to the smoke-point height. The sooty aromatic fuels on the right have high TSI values and correspondingly low smoke-point heights. Olson's faired-curve approximates our previous scaling predictions, Eq. 6,

$$(k_s)_{\text{smoke point}} \sim \ell_{fs}^{-1/2} \sim (\text{TSI})^{1/2} .$$

Similar scaling relationships are obtained by Kent and Wagner[21].

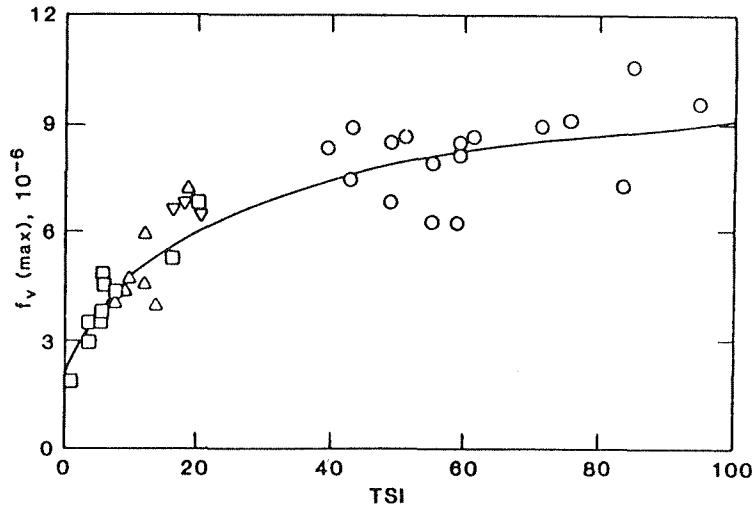

□ = alkanes; Δ = alkenes; ∇ = alkynes; O = aromatics.

Fig. 8: Comparison of maximum soot concentration and soot threshold i diffusion flames

e) Pressure Scaling and Soot Reaction Order - The scaling relatior ships can be extended to other than atmospheric pressure. During th 1950's Schalla and McDonald[22] measured the smoke-points for a variet of liquid fuels over an eight-fold absolute pressure range. They four that the product of the absolute pressure and smoke-point height is pre cisely constant.

$$\ell_{fs} P = \text{const} \qquad (8$$

Examination of our flame height formula (4) and the velocity and flan radius results (1a) and (1b) yield the following pressure dependencies

$$\ell_f \sim \dot{Q}_{TOT} P^o, \qquad r_f^2 \sim \ell_f^{1/2} P^{-1}, \qquad \tau_f \sim \ell_f / u_f \sim \ell_f^{1/2} P^o \qquad (9a,9b,9c$$

since the product of $\rho_f \nu_f$ is independent of pressure.

Our previously established arguments, (following Eq. (7)), for radia tive fractions from smoke-point flames presumed a general similarity c flame temperatures for smoke-point flames involving fuel/oxidant combina tions with similar adiabatic stoichiometric flame temperatures. It i anticipated that, in a similar manner, these flame temperatures are inde pendent of pressure, so that from Eq. (7)

$$\chi_{Rs} = \frac{\dot{Q}_{Rs}}{\dot{Q}_{TOT}} \sim \frac{k_{sp} \ell_{fs} r_f^2}{\dot{Q}_{TOT}} \sim k_{sp} \ell_{fs}^{1/2} / P \qquad (10$$

after substituting from Eq.'s (9a) and (9b) for $\dot{Q}_{TOT}$ and r_f^2.

Now we can address the effective soot formation/oxidation reactic order by blithly assuming both the soot formation and oxidation rate have the same order, n, and examine the consequences of the assumptior Thus defining a general soot reaction rate function f, one has

$$\frac{Dk_s}{Dt} = \frac{D(\rho Y_s)}{Dt} = P^n f(Y_i, T) \qquad (11)$$

where Y_s is the soot mass fraction, Y_i and T are the local compositions and temperature, while f is independent of pressure. Invoking once again our general similarity assumption, we have

$$\frac{Dk_s}{Dt} \simeq \frac{k_{sp}}{\tau_{fs}} \sim \frac{k_{sp}}{\ell_{fs}^{1/2}} \sim \frac{\chi_{Rs} P}{\ell_{fs}} \sim \chi_{Rs} P^2 \qquad (12)$$

where we use in sequence Eq. (9c) for τ_{fs} and Eq. (10) for k_{sp} and finally the empirical relationship (8) for ℓ_{fs}.

It appears quite likely that the radiant fraction χ_{Rs} is independent of pressure although this has not been experimentally verified. If this is the case then comparison of Eq. (11) and (12) suggests that the effective combined soot formation/oxidation rate is second order in pressure. Upon reflection such a second order dependence would not be surprising for both soot formation and oxidation.

In the case of soot formation various proposed detailed chemical mechanisms[25] all involve bimolecular exchange reactions so this result is anticipated. On the other hand soot oxidation in rich regions probably occurs primarily by hydroxyl radical attack on the soot particles[24] which in itself is likely to be a first order surface reaction. However, the hydroxyl radical concentration is probably pressure dependent so that the actual controlling reactions for soot oxidation may nevertheless occur in the gas phase. Fenimore[23] has shown that soot oxidation rates are very similar to CO oxidation rates and they both occur in the same flame regions. A sequence of bimolecular exchange reactions for CO oxidation must generate an extra free radical for each oxidation of a carbon monoxide molecule. For example, an overall sum of bimolecular exchange reactions might produce the result

$$2CO + O_2 + H_2O \rightarrow 2CO_2 + OH + H$$

which preserves the total number of molecules on both sides. These resulting generated free radicals would then be available for soot oxidation.

The above discussion is presented with the intent of merely showing that it is possible that both the soot formation and oxidation processes can be controlled by second order reactions. Partial confirmation of this result could be obtained by adding to the fuel trace amounts of salts which are known to significantly increase the number of soot particles and soot surface area without altering the soot volume fraction. If the smoke-point of a fuel were essentially unaffected by the addition of trace amounts of salts, one might then conclude that soot oxidation rates in diffusion flame were controlled by gas phase rather than surface reactions.

FLAME RADIATION TEST METHOD

It is clear from the preceding discussion that a fuel's smoke-point represents its key measurable property which controls its flame radiation and consequent large-scale fire hazard. Smoke-point heights can be readily measured for gaseous fuels (fuel jets) and liquid fuels (wick bur-

ner). Solid fuels present a more formidable challenge. They general produce a protective char layer which induces transient burning. The require high incident radiant fluxes to induce pyrolysis. Such fluxe must not interfere with the combustion or any flame radiation measure ments. The pyrolysis vapors must be prevented from any unwanted therm cracking through contact with heated surfaces before entering the diff sion flame. Finally, the apparatus must be convenient to operate[26].

Several investigators are now exploring possible smoke-point te methods. Figure 9 shows an apparatus being assembled at FMRC. It is lates the pyrolysis chamber from the flame region and uses a protecti gas shield to prevent unwanted surface heating of the pyrolysis vapo before they enter the flame.

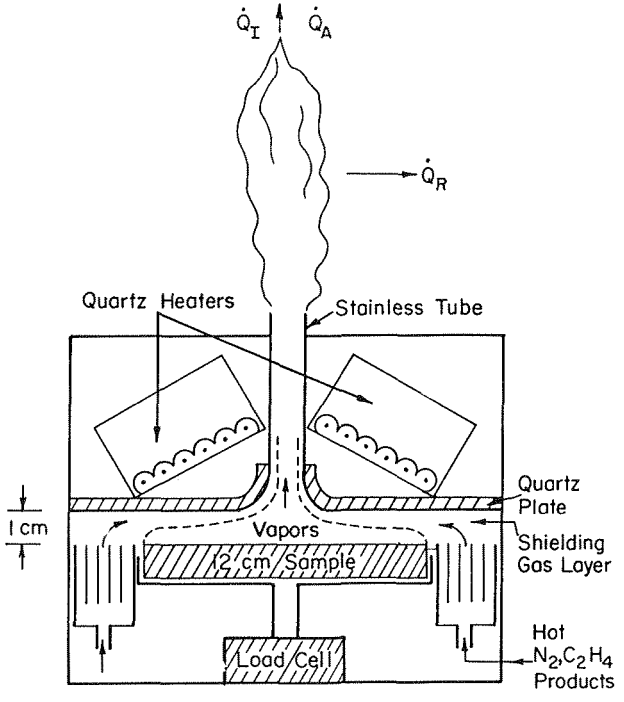

Fig. 9: Flame radiation test apparatus being assembled at FMRC

CONCLUSIONS

We have briefly reviewed a few of the important available materi flammability tests. At present we do not have available a suitable te for inferring the radiative properties of flames produced by solid fuel These flame radiation properties unfortunately control large-scale fi hazards. Careful measurements of the radiation from large-scale turb lent flames show that flame radiation is closely correlated by the cla

sical smoke-point values. We next summarize many recent discoveries on the scaling of soot formation and radiation from buoyant laminar diffusion flames. The numerous correlations suggest that a fuel's smoke-point plays a fundamental role in controlling flame radiation and smoke output. It may also control the emission of toxicants such as unburned hydrocarbons and carbon monoxide. We have pointed out some of the problems to be overcome in the development of an apparatus for the measurement of the smoke-point of solid fuels. A possible apparatus is presented. Finally, it is apparent that our empirical understanding of flame radiation and soot-formation is advancing very rapidly and is now available for supporting the development of a general scientific understanding and models of flame radiation processes.

NOMENCLATURE

B	B-Number
C	Specific heat, J/gK
d_s	Thin-fuel thickness, m
D_f	Species diffusivity at flame temperature, m^2/s
f	Function
f_v	Soot volume fraction
F^2	Ratio of inertia and buoyancy forces
g	Acceleration of gravity, m/s^2
$G(s)$	Function
$h^{(o)}$	Natural convection coefficient, J/m^2Ks
ΔH_c	Heat of combustion
k	Absorption emission coefficient, m^{-1}
k	Thermal conductivity, J/m Ks
ℓ_f	Flame height, m
ℓ_{fs}	Smoke-point flame height, m
$\dot{m}''$	Mass transfer, g/m^2s
$\dot{m}''_F$	Fuel consumption rate per unit flame area, g/m^2s
$\dot{M}_F$	Fuel (undiluted) supply rate, g/s
M	Molecular weight
P	Pressure, g/ms^2
$\dot{q}''$	Heat transfer rate per unit area, J/m^2s
$\dot{Q}_R$	Total flame radiant emission, J/s
r_f	Characteristic flame radius, m
R	Ratio of inertia to viscous forces
s	Stoichiometric oxidant/fuel mass ratio
t	Time
T	Temperature
u_f	Characteristic buoyant velocity, m/s
V	Spread rate, m/s

V_g Gas velocity, m/s

Y_{fT} Concentration of fuel from supply port

ν' Stoichiometric coefficient

ν_f Kinematic viscosity, m^2/s

ρ_f Density at flame temperature, g/m^3

τ_f Characteristic flow time, s

χ_R Radiant fraction

σ Stefan-Boltzmann constant, J/m^2sK^4

Subscripts

F Fuel
f flame
g Gas
s soot, solid, smoke-point
O oxidant
∞ Ambient
ig ignition

REFERENCES

1. Pagni, P.J. and Shih, T.M.: "Excess Perolycate," Sixteenth Symposiu (International) on Combustion, pp 1329-43, The Combustion Institute Pittsburgh (1976)

2. Delichatsios, M.A.: "Modeling of Aircraft Cabin Fires," FMR Technical Report RC84-BT-10, Factory Mutual Research Corporation Norwood, MA, (May 1984).

3. de Ris, J: "Fire Radiation - A Review," pp 1003-15, Seventeenth Sym posium (International) on Combustion. The Combustion Institute Pittsburgh, PA (1979).

4. Modak, A.T.: "Radiation from Products of Combustion," Fire Researc 1, (1978/79) 339-361.

5. Grosshandler, W.L.: "Radiative Heat Transfer in Nonhomogeneous Gases A Simplified Approach," Int. J. Heat Mass Transfer, Vol. 23, pp 1447 59, (1980).

6. Grosshandler, W.L. and Modak, A.T.: "Radiation from Nonhomogeneou Combustion Products," Eighteenth Symposium (International) on Combus tion, The Combustion Institute (1981)

7. Modak, A.T. and Mathews, M.K.: "Radiation Augmented Fires Withi Enclosures," Journal of Heat Transfer, 100, pp 544-7, (1978)

8. Hottel, H.C. and Sarofim, A.F.: "Radiative Transfer," McGraw Hill (1967).

9. de Ris, J.: "Buoyant Diffusion Flames," Heat Transfer and Buoyan Convection (D.B. Spalding and H.H. Afgan, Eds) pp 813-31, Hemispher Publ. (1977).

10. Santo, G. and Tamanini, F.: "Influence of Oxygen Depletion on the Radiative Properties of PMMA Flames," pp 619-31, Eighteenth Symposium (International) on Combustion, The Combustion Institute, Pittsburgh, PA (1981).

11. Markstein, G.H.: "Relationship Between Smoke Point and Radiant Emission from Buoyant Turbulent and Laminar Diffusion Flames," Twentieth Symposium (International) on Combustion, (in press).

12. Markstein, G.H.: "Measurements on Gaseous-Fuel Pool Fires with a Fiber-Optic Absorption Probe," Comb. Sci. and Tech., 39, 215-33, (1984).

13. Roper, F.G.: Combustion and Flame, 29, pp 219-26, (1977).

14. Schug, K.P., Manheimer-Timnat, Y., Yaccarino, P., and Glassman, I.: "Sooting Behavior of Gaseous Hydrocarbon Diffusion Flames and the Influence of Additives," Comb. Sci. and Tech., 22, pp 235-50, (1980).

15. Roper, F.G., Smith, C., and Cunningham, A.C.: Combustion and Flame, 29, pp 227-34, (1977).

16. Glassman, I. and Yaccarino, P.: Comb. Sci. and Tech., 24, pp 107-14 (1980).

17. Markstein, G.H.: Unpublished work.

18. Markstein, G.H. and de Ris, J.: "Radiant Emission and Absorption by Laminar Ethylene and Propylene Diffusion Flames," Twentieth Symposium (International) on Combustion, (1985).

19. Olson, D.B.: "Soot Formation in Synfuels," AeroChem TP-433, Aero Chem Res. Labs, Princeton, NJ (1983)

20. Markstein, G.H.: "Radiant Emission and Smoke Points for Laminar Diffusion Flames of Fuel Mixtures," Eastern Section of The Combustion Institute, (Dec. 1984).

21 Kent, J.H. and Wagner, H.Gg.: "Temperature and Fuel Effects in Sooting Diffusion Flames," Twentieth International Symposium on Combustion (1985).

22. Schalla, R.L. and McDonald, G.F.: "Mechanism of Smoke Formation in Diffusion Flames," pp 316-24, Sixth Symposium (International) on Combustion, (1956).

23. Fenimore, C.P. and Jones, G.W.: "Coagulation of Soot to Smoke in Hydrocarbon Flames," Combustion and Flame, 13, pp 303-10 (1970).

24. Neoh, K.G.: "The Study of Soot Burnout in Flames," Ph.D. Thesis, M.I.T. (1981).

25. Frenklach, M. and Clary, D.W.: "Detailed Kinetic Modeling of Soot Formation in Shock Tube Pyrolysis of Acetylene," Twentieth Symposium (International) on Combustion, (1985).

26. de Ris, J.: "Flammability Testing, State-of-the-Art" Fire and Materi
als (in press) also FMRC Technical Report RC83-BT-7.

27. Orloff, L., de Ris, J., and Markstein, G.H.: "Upward Turbulent Fir
Spread and Burning of Fuel Surfaces," Fifteenth Symposium (Interna
tional] on Combustion, pp 183-92, The Combustion Institute, Pitts
burgh (1975).